IEEE Access
Multidisciplinary | Rapid Review | Open Access Journal

Received 15 June 2024, accepted 8 July 2024, date of publication 15 July 2024, date of current version 23 July 2024.

Digital Object Identifier 10.1109/ACCESS.2024.3427728

RESEARCH ARTICLE

Traceback Analysis of Unknown Nanoparticles Formation Mechanism on OSP Surface Finished PCB for Flip-Chip Package

HA-YEONG KIM[1], JIWON KIM[1], YEON-RYONG CHU[1], SUK JEKAL[1], MINKI SA[1], CHAN-GYO KIM[1], GYU-SIK PARK[2], JISU LIM[2], ZAMBAGA OTGONBAYAR[1], AND CHANG-MIN YOON[1]

[1]Department of Chemical and Biological Engineering, Hanbat National University, Daejeon 34158, South Korea
[2]Department of Intelligent Nano Semiconductor, Hanbat National University, Daejeon 34158, South Korea

Corresponding authors: Zambaga Otgonbayar (zambaga@hanbat.ac.kr) and Chang-Min Yoon (cmyoon4321@hanbat.ac.kr)

This work was supported in part by the Development of High-Power Supercapacitor Research and Development Program of the Ministry of Trade, Industry and Energy/Korea Planning & Evaluation Institute of Industrial Technology (MOTIE/KEIT), Development of Lithium-Ion Capacitors for the Control of Load Variation of Hydrogen Vehicles, in 2024, under Grant 00156073; and in part by the Challengeable Future Defense Technology Research and Development Program through the Agency For Defense Development (ADD) funded by the Defense Acquisition Program Administration (DAPA), in 2024, under Grant 915066201.

ABSTRACT In this paper, we present the concept of traceback analysis to identify the origins of non-wet defects caused by hydrophobic unknown nanoparticles in the semiconductor packaging process. Traceback analysis involves five-steps, *i.e.*, practical observation of failure mode, detailed physical and chemical analysis, process investigation, hypothesis establishment, and failure reproduction with comparison. Initially, the morphology and composition of the unknown nanoparticles are analyzed using an optical microscope (OM), field-emission scanning electron microscopy (FE-SEM), contact angle (CA), energy-dispersive spectroscopy (EDS), and Fourier-transform infrared spectroscopy (FT-IR). As a result, spherical unknown nanoparticles with a size of *ca.* 500 nm consists of organic imidazole-derived materials, similar to the composition of organic solderability preservative (OSP). To identify the origin, printed circuit board (PCB) manufacturing processes are reviewed step-by-step. Traceback analysis identifies that the 1-methoxy-2-propyl acetate (PGMEA) cleaning solvent can form spherical emulsions when mixed with deionized (DI) water during the cleaning process. This can occur when PGMEA and DI water mix in the cleaning bath or recycling pipes, or when leftover PGMEA and DI water mix during next cleaning processes. These PGMEA/DI water form emulsions owing to the polarity differences between hydrophobic PGMEA and hydrophilic DI water and remain on the PCB surface. Thus, organic nanoparticles grow in the PGMEA emulsion on the Cu pad during OSP application for surface finishing purposes. This comprehensive approach ensures a thorough understanding of defect origins. The traceback analysis described in this study, involving five-steps, is applicable not only in semiconductor packaging but also in defect investigation across various industries.

INDEX TERMS Non-wet, OSP, traceback analysis, emulsion, PCB.

I. INTRODUCTION

Flip-chip packaging is one of the most widely employed first-level interconnection techniques for integrated circuit (IC) chips [1]. The pattern or active side of the IC for the flip-chip package faces down to connect to the printed circuit board (PCB) substrate [2]. In comparison to conventional wire bonding technology, flip-chip packages possess various advantages, *i.e.*, increased I/O count density, shorter interconnection path, improved thermal dissipation, and faster processing time [3]. This flip-chip technology was first introduced by International Business Machines

The associate editor coordinating the review of this manuscript and approving it for publication was Woorham Bae.

© 2024 The Authors. This work is licensed under a Creative Commons Attribution-NonCommercial-NoDerivatives 4.0 License.
For more information, see https://creativecommons.org/licenses/by-nc-nd/4.0/

Corporation (IBM) in the form of a C4 (controlled-collapse chip connection) solder bump [1], [4]. After C4 technology, generations have evolved into C2 (chip connection) solders formed on copper pillars or posts [5]. For the flip-chip mount, solder bumps were thermally connected to the pad of the substrate PCB *via* a reflow process [1].

To ensure the reliability of the interconnection, surface-finishing methods were introduced for the pad of the PCB substrate. One of the most extensively employed methods is gold (Au) - based surfaces, which include electroless nickel immersion gold (ENIG) and electroless nickel electroless palladium immersion gold (ENEPIG) [6]. Owing to its high electrical conductivity and chemical resistance, Au is a preferable noble metal in the electronics industry, especially in semiconductor fabrication, which requires high reliability [7], [8]. However, high cost is one of the few disadvantages of gold, along with its low refined yield [9]. Therefore, researchers have focused on other surface finishes using metals like silver (Ag), tin (Sn), and copper (Cu) as the interconnection pad of the PCB substrate [10]. Despite their cost advantage, these metals suffer from natural oxidation, resulting in degraded electrical performance [11]. Therefore, research has been conducted to prevent oxidation by using various methods and chemicals.

Among other metals, Cu has distinct advantages over Au in various aspects, such as higher electrical conductivity, thermal conductivity, and lower cost [12], [13]. Moreover, Cu has a high oxidation level. Nevertheless, oxidation is suppressed in a stable environment; thus, thin metals are coated on the main Cu components. Furthermore, organic finishing methods have been developed to prevent oxidation of the interconnection pads of PCB substrates. For Cu metal, the organic solderability preservative (OSP) was composed of imidazole-derived benzimidazole [14]. These OSP methods have the advantages of simple and fast processing, effective oxidation protection, and enhanced wettability [15]. However, unwanted side reactions may occur during the PCB and OSP surface finishing processes in the presence of chemicals, solvents, and surfactants. Unwanted reactions may produce organic residues or particles, even in the nano-size range, thus decreasing the wettability between the pad and solder bump and causing non-wet failure [16].

In this study, we focused on the non-wet failure of an OSP-finished flip-chip package. Our SEM analysis clearly showed that unknown nanoparticles were present on the surface of the OSP-coated copper (Cu) pads. With traceback analysis and engineering, the root and cause of unknown nanoparticles were discussed in a step-by-step manner through the investigation of the synthesis and surface finishing of the OSP-applied PCB from the perspective of the chemical reactions of the materials. Moreover, unknown nanoparticles were produced from the reactions of chemicals and solvents employed in practical PCB manufacturing processes. The objective of our study was not only limited to the examination of unknown nanoparticles causing non-wet failure in the flip-chip to OSP-finished substrate PCB, but also to the general strategy for resolving the production of unwanted nanoparticles in view of the chemical reaction.

We propose a precise expression for the main findings of this study in four flows.

- We find that the unknown nanoparticles on the Cu pad in flip-chip package causing the non-wet failure by lowering the solderability between solder bump and Cu pad.
- We use various analytical methods to determine the morphology and chemical structures of unknown nanoparticles.
- We confirm the associated PCB manufacturing processes by step-by-step manner and conduct the reproduction experiments, verifying the formation mechanism of unknown nanoparticles.
- We discuss the successful application of traceback analysis to solve the cause of non-wet failure by the unknown nanoparticles. This traceback analysis and its five-step methodology can be applied to solve other failures in the semiconductor packaging process.

II. EXPERIMENTS

A. MATERIALS

1-methoxy-2-propyl acetate (PGMEA, $CH_3CO_2CH(CH_3)CH_2OCH_3$, 99.0%), ammonium hydroxide solution (NH_4OH, 28.0–30.0%), acetic acid (CH_3COOH, 99.5%), and copper (I) chloride (CuCl, 93.0%) were purchased from Samchun Chemical Co., LTD (Seoul, Korea). Isopropyl alcohol (IPA, $(CH_3)_2CHOH$, 99.5%) was purchased from Duksan Pure Chemicals Co., LTD (Ansan, Korea). Benzimidazole ($C_7H_6N_2$, $>$ 98.0%) and ethylenediaminetetraacetic acid (EDTA, $>$ 98.0%) were purchased from Tokyo Chemical Industry Co., LTD (Tokyo, Japan). All chemicals were used without further purification.

B. PREPARATION OF OSP SOLUTION

Benzimidazole (1.0 g) was dispersed in CH_3COOH (1.92 mL) and stirred for 1 h at room temperature (25 °C). CuCl (0.04 g) was added to NH_4OH (0.67 mL) and the mixture was stirred for 1 h at room temperature. Both solutions were mixed with deionized (DI) water (100 mL) and stirred for 1 h. Subsequently, EDTA (0.02 g) was added to the mixture; the reaction proceeded for 12 h with magnetic stirring at room temperature to obtain the OSP solution. The OSP solution was then coated onto the surface of Cu pad to prevent oxide layer formation.

C. REPRODUCTION OF UNKNOWN NANOPARTICLES

To confirm the miscibility and emulsion formation, PGMEA and IPA were mixed in deionized (DI) water at three different concentrations (1, 10, and 20 wt%) in a final volume of 20 mL and magnetically stirred for 5 min at room temperature. The OSP solution (2.0 mL) was injected into the

as-prepared PGMEA and IPA mixed solvent and stirred for 10 h at 400 rpm. After the reaction, the OSP-injected PGMEA and IPA solutions were centrifuged to collect the precipitates or unknown nanoparticles, and the supernatants were discarded. The collected precipitates were dried in an oven overnight at 60 °C.

D. CHARACTERIZATION

The appearance of non-wet failure of the flip-chip package was observed using an optical microscope (OM, BH2-UMA, Olympus). The morphologies of the OSP-finished Cu pad with unknown nanoparticles and reproduced nanoparticles on the PCB were evaluated using field-emission scanning electron microscopy (FE-SEM, S-4800, Hitachi). The elemental compositions were obtained using an energy-dispersive spectrometer (EDS, Elect Super, AMETEK) installed in the FE-SEM. The surface properties of the pristine Cu pad, OSP-finished Cu pad, and OSP-finished Cu pad with unknown nanoparticles were investigated using contact angle measurements (CA, Phoenix 300, SEO). The chemical structure bonds of the OSP-finished Cu pad with unknown nanoparticles were investigated using Fourier-transform infrared spectroscopy (FT-IR, Nicolet iS10, Thermo Fisher Scientific).

III. RESULTS AND DISCUSSION

A. PRACTICAL OBSERVATION OF FAILURE MODE

The actual failure of non-wetting caused by the unknown nanoparticles in the semiconductor packaging process was confirmed. Fig. 1a illustrates a cross-sectional view of the flip-chip package. The patterned side of the IC chip was connected to the PCB substrate *via* an interconnection between the solder bump and the Cu pad. OM analysis was conducted to confirm the practical non-wet failure, which is one of the most common failures in flip-chip packages, as shown in Fig. 1b. Numerous factors, including the temperature profile, warpage of materials, and low wettability, can cause non-wet failure of solder bumps on the Cu pad. In terms of wettability, the presence of organic materials or contaminants directly degrades the soldering between the bump and pad, resulting in non-wet failure. To closely examine the morphology of the unknown nanoparticles, FE-SEM was conducted on the PCB, which revealed non-wet failure, as shown in Fig. 1c. The size of the unknown nanoparticles was determined to be *ca*. 500 nm; and their shape was spherical. The effects of the unknown nanoparticles on the surface properties of the Cu pad were investigated using CA measurements (Fig. 2). The contact angles of various PCB substrates with pristine, OSP-finished, and OSP-finished

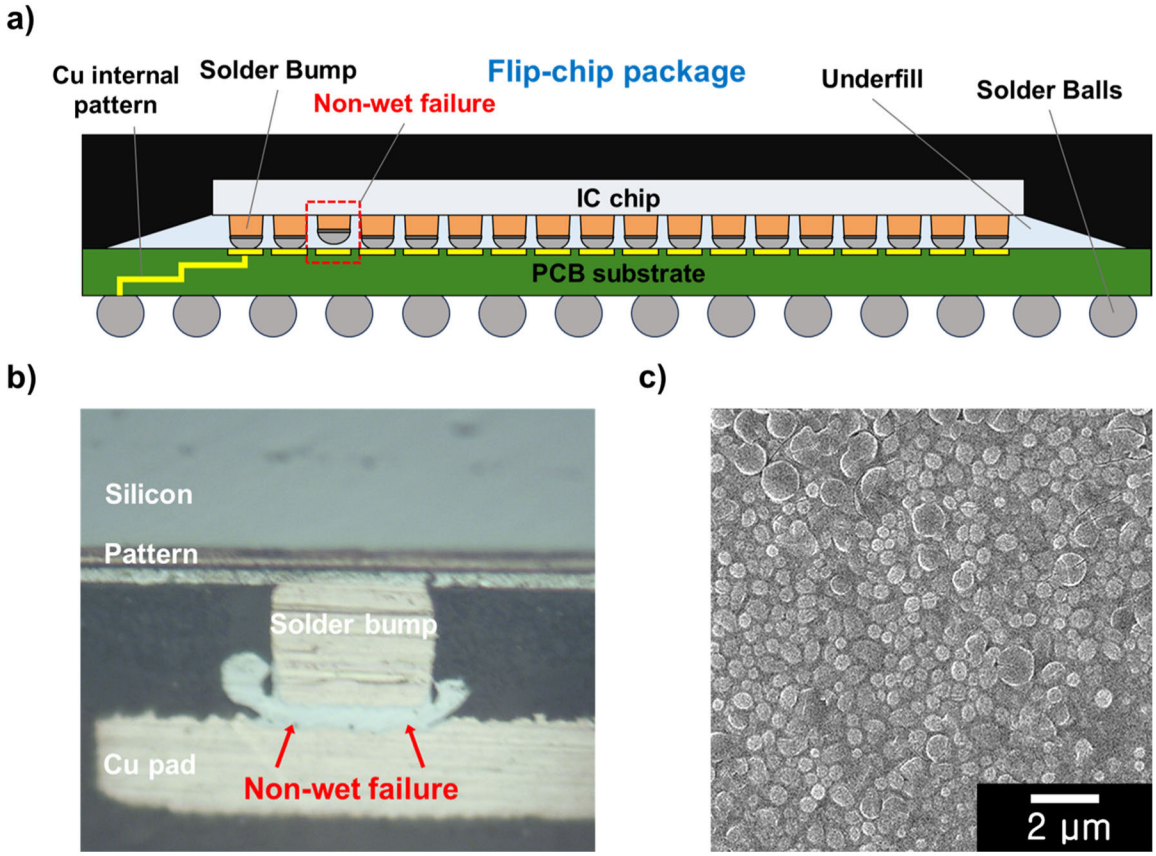

FIGURE 1. a) Schematic illustration of flip-chip package. b) OM image of non-wet failure in flip-chip package at solder bump and Cu pad of PCB substrate. c) SEM image of unknown nanoparticles formed on the Cu pad of OSP-finished PCB substrate.

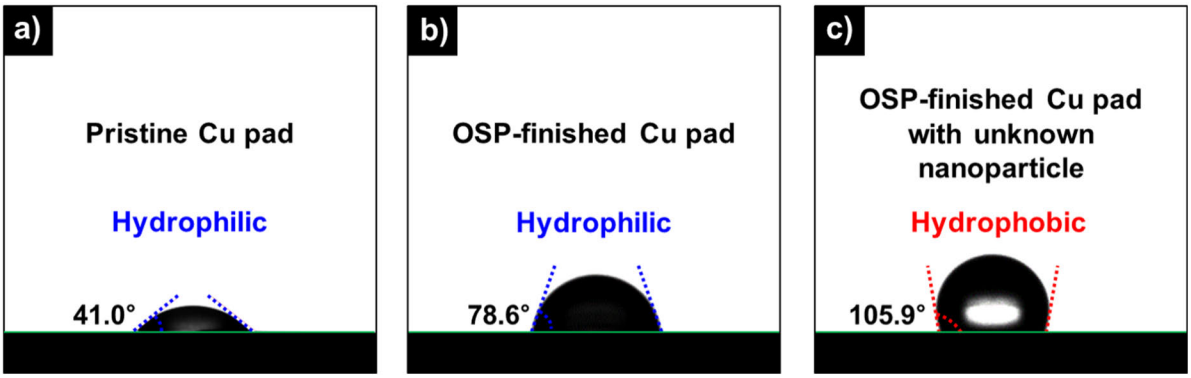

FIGURE 2. CA images of water droplet on surface of a) pristine Cu pad, b) OSP-finished Cu pad, and c) OSP-finished Cu pad with unknown nanoparticles.

Cu pad with unknown nanoparticles were measured to be *ca.* 41.0°, 78.6°, and 105.9°, respectively. We clearly observed that the pristine Cu pad exhibited the most hydrophilic properties without organic materials. With OSP finishing, the contact angle of the Cu pad increased owing to the hydrophobic properties of the OSP. Notably, the PCB substrate with unknown nanoparticles exhibited the highest hydrophobicity, which might impede metal-to-metal bonding during the reflow process and lead to non-wet failure.

B. DETAILED PHYSICAL AND CHEMICAL ANALYSIS

Various detailed analyses were conducted to confirm non-wet failure. First, EDS was conducted on an OSP-finished Cu pad with unknown nanoparticles to investigate their elemental composition. For the OSP-finished Cu pad, C, O, N, and Cu were detected. In addition, the OSP-finished Cu pad with unknown nanoparticles contained C, O, N, and Cu, similar to the OSP-finished Cu pads with different elemental ratios. Importantly, only C, O, and N were detected as non-metals, indicating that the majority of the organic materials or solvents utilized did not contain other elements. The elemental compositions of the OSP-finished Cu pad and the OSP-finished Cu pad with unknown nanoparticles are shown in Fig. 3a.

FT-IR analysis was used to characterize the chemical structures of the OSP-finished Cu pad and the OSP-finished Cu pad with unknown nanoparticles (Fig. 3b). For the OSP-finished Cu pad, peaks related to benzimidazole and copper oxide were mainly detected. In detail, the peaks observed at 3,100–2,980 cm^{-1} indicate aromatic C–H and N–H stretching [17]. In addition, the peak observed at 1,613 cm^{-1} corresponds to N–H bending [18], [19], [20], [21]. The peaks at 1,551 and 1,499 cm^{-1} were attributed to the presence of C = N stretching vibrations [22]. Moreover, aromatic C–N stretching peaks were observed at 1,247 cm^{-1} [23]. These peaks clearly demonstrated that benzimidazole or derived materials containing amine and imine groups were the main chemicals in the OSP-finished Cu pad (Fig. S1). Furthermore, peaks ascribed to the slightly formed oxide layer on the Cu pad were observed at 1,464 and 1,303 cm^{-1} and were attributable to Cu–O structures [24]. For the OSP-finished Cu pad with unknown nanoparticles, similar N-related characteristic peaks were observed at 3,057, 1,603, 1,342, and 1,247 cm^{-1} and were attributed to C–H and C–N stretching, N–H bending, C–N stretching, and aromatic C–N stretching, respectively [25], [26]. In addition, other peaks, including O–H stretching, C–O stretching, and C = C bending, were detected at 3,300, 1,180, 1,113, 1,004, and 964–905 cm^{-1}, indicating the presence of organic materials other than N-related materials in both the OSP-finished Cu pad and the OSP-finished Cu pad with unknown nanoparticles [27], [28], [29], [30]. Moreover, small traces of Cu–O materials were detected at 1,464 and 1,303 cm^{-1} in analogous to the OSP-finished Cu pad [31], [32].

C. INVESTIGATION OF PROCESS

To better understand the origin of the unknown nanoparticles, the manufacturing process of the OSP surface-finished PCB and the utilized chemical materials were investigated. The manufacturing process of PCB involves many steps, such as printing, etching, lay-up, drilling, electroless deposition, imaging of the outer layer, plating, solder mask coating, and surface finishing (Fig. 4a) [33]. Furthermore, cleaning process is frequently performed during many processes to remove dust and residues. Therefore, cleaning solvents such as IPA, PGMEA, alcohol mixtures, and DI water have been utilized for cleaning processes in various manufacturing industries [26], [34]. For the PCB cleaning process, the PCB was placed in a cleaning bath and the cleaning solvent or DI water was sprayed for cleaning (Fig. 4b) [35]. During the cleaning process, cleaning solvents with dirt are recycled directly from the cleaning bath or some filtrations are applied before recycling. These recycling of cleaning solvents is essential from the perspective of cost reduction, but there is also the risk of mixing leftover solutions from the cleaning process within the bath or pipes.

D. HYPOTHESIS ESTABLISHMENT

Leftover PGMEA or IPA can be mixed with DI water for a sequential cleaning process. Therefore, different molecular

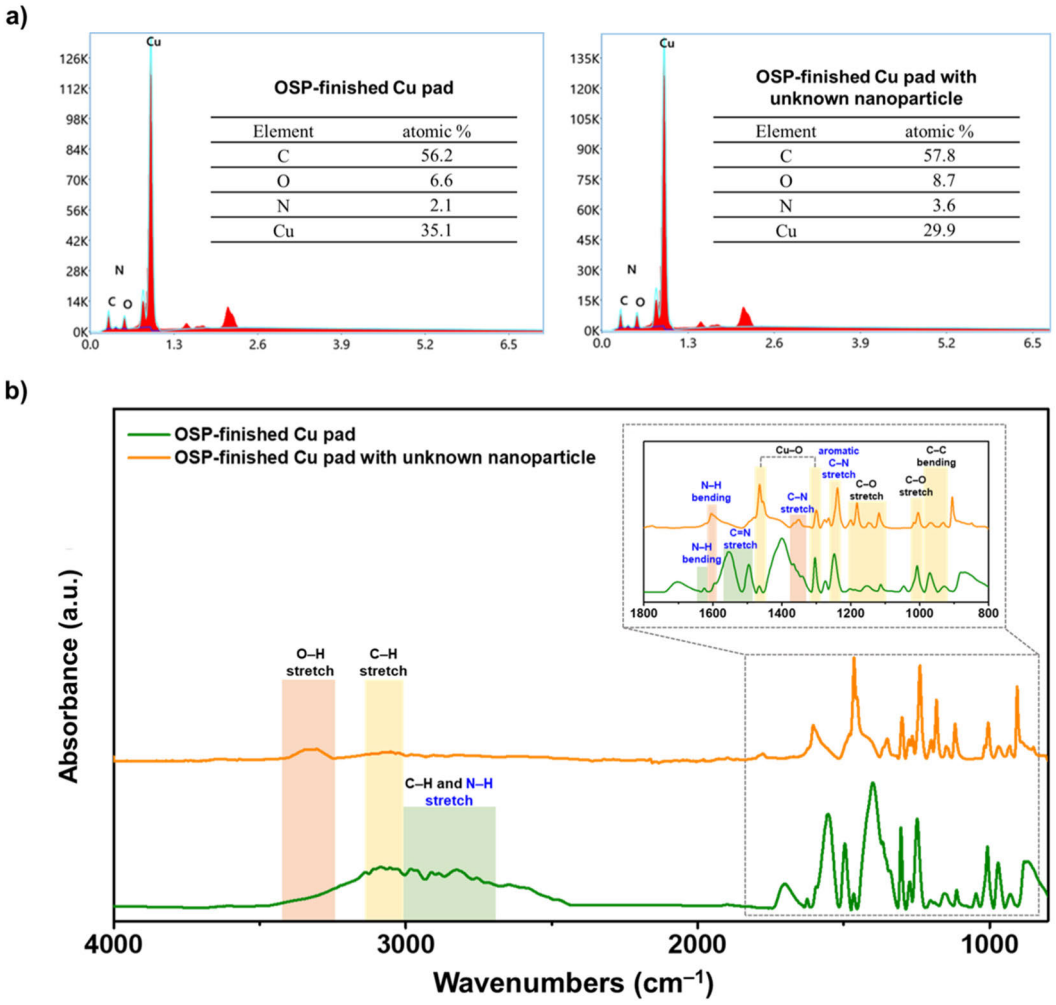

FIGURE 3. a) EDS spectra and b) FT-IR spectra of OSP-finished Cu pad and OSP-finished Cu pad with unknown nanoparticles.

sizes of cleaning solvents may impact their ability to mix with DI water. Solvents with smaller molecules, such as IPA, were miscible with DI water; however, PGMEA, owing to its larger molecular size, displayed lower miscibility.

To observe the miscibility, the IPA and PGMEA solvents were mixed with DI water at three different concentrations: 1, 10, and 20 wt%. We clearly observed that all concentrations of IPA solvents were homogeneously mixed without any separation with DI water. In contrast, PGMEA solvents were composed of non-homogeneous mixtures in DI water. Furthermore, emulsions were formed in PGMEA/DI water mixtures with concentrations of 10 and 20 wt% (Fig. 5a). In addition, the laser irradiated the IPA and PGMEA/DI water mixtures at 20 wt%, and light scattering occurred only in the PGMEA/DI water mixture owing to the presence of the emulsion (Fig. 5b). The formation of emulsions originated from the molecular structure and relatively nonpolar nature of PGMEA in DI water. In general, solvent mixtures with different polarities, assisted by hydrodynamic forces, can produce emulsions [36]. Thus, in practical cleaning processes, a relatively nonpolar PGMEA solvent can aggregate in polar DI water with the assistance of stirring or even flowing conditions. One of the most interesting functions of an emulsion is its capacity as a nanoreactor for nanoparticles [37]. Thus, we hypothesized that PGMEA and the emulsion may be related to the formation of unknown nanoparticles. In addition, the aforementioned OSP, which was analogous to the elemental and chemical compositions of the unknown nanoparticles, was correlated with the cleaning solvents.

With regard to the origin of the unknown nanoparticles, we hypothesized that the emulsions formed by PGMEA in DI water act as nanoreactors for the growth of spherical nanoparticles based on OSP (Fig. 6a).

E. REPRODUCTION OF FAILURE WITH COMPARISON

To verify our hypothesis, OSP was added to PGMEA/DI water mixtures at three different concentrations. Additionally, OSP was added to the IPA/DI water mixture for comparison purposes. OSP was then injected into the mixture and stirred

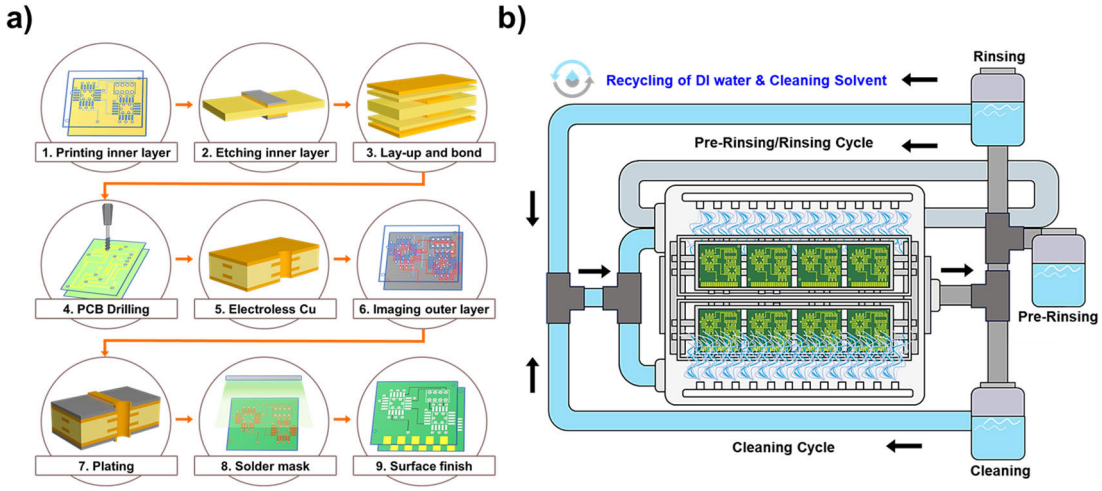

FIGURE 4. Schematic illustration of a) PCB manufacturing process and b) PCB washing showing the recycling of DI water and cleaning solvent during the process.

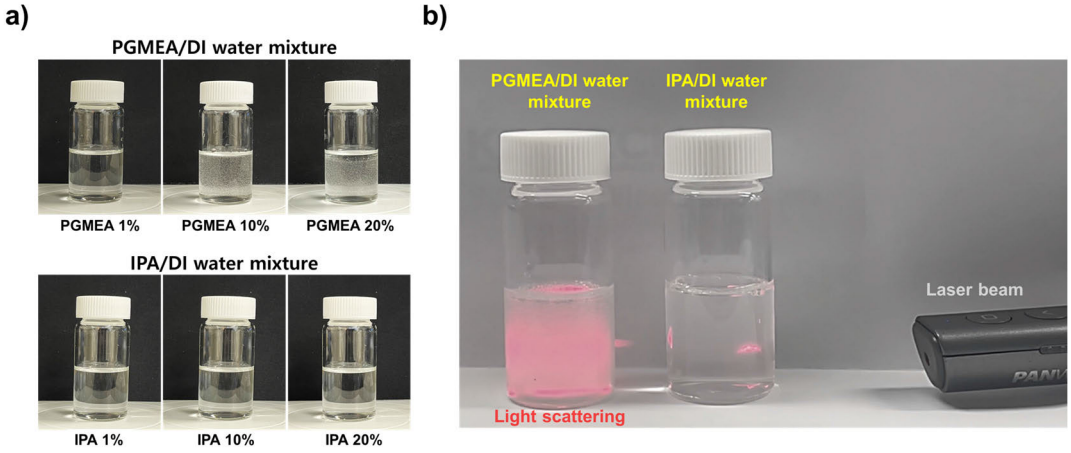

FIGURE 5. Digital photographs of a) PGMEA and IPA solvents in DI water at 1, 10, and 20 wt% concentrations and b) light scattering results of PGMEA and IPA solvents (20 wt%) using a laser beam.

at a constant speed for 10 h at room temperature (Fig. 6b). After the reaction, the solutions were drop-cast for FE-SEM analysis (Fig. 7). Notably, spherical OSP-injected PGMEA-based nanoparticles (OSP/PGMEA-NPs) with a size of *ca.* 500 nm were obtained from the sampling of OSP-injected PGMEA mixtures of 10 and 20 wt%. In contrast, residues with no morphology or aggregates were observed in the OSP-injected IPA mixtures. Clearly, the solutions with emulsions formed only spherical nanoparticles, which was in accordance with our hypothesis. Accordingly, our final task was to compare the reproduced OSP/PGMEA-NPs with the OSP-finished Cu pad with unknown nanoparticles. In this regard, EDS and FT-IR analysis were performed on the OSP/PGMEA-NPs and OSP-finished Cu pad with unknown nanoparticles. First, EDS was employed to quantify the elemental compositions of the samples, as listed in Table 1. We clearly observed that both samples exhibited similar compositions, thus verifying the presence of N element from the imidazole-based materials in OSP. Furthermore, the FT-IR spectra of the OSP/PGMEA-NPs and OSP-finished Cu pad with unknown nanoparticles provided detailed information regarding the similarities in their chemical and molecular structures, as shown in Fig. 8. Both materials exhibited N-related peaks at 1,603, 1,342, and 1,247 cm^{-1}, indicating N–H bending, C–N stretching, and aromatic C–N stretching vibrations, respectively [38], [39], [40], [41]. In addition, characteristic peaks associated with organic compounds were observed at 3,057, 1,180–1,004, and 964–905 cm^{-1}, corresponding to C–H stretching, C–O stretching, and C = C bending vibrations, respectively [42], [43]. Moreover, Cu–O peaks were detected at 1,464 and 1,303 cm^{-1} for both the OSP/PGMEA-NPs and OSP-finished Cu pad with unknown nanoparticles [23]. Consequently, the OSP/PGMEA-NPs and OSP-finished Cu pad with unknown nanoparticles were analogous in terms of morphology, size, elemental composition, and chemical structure, thus confirming that the

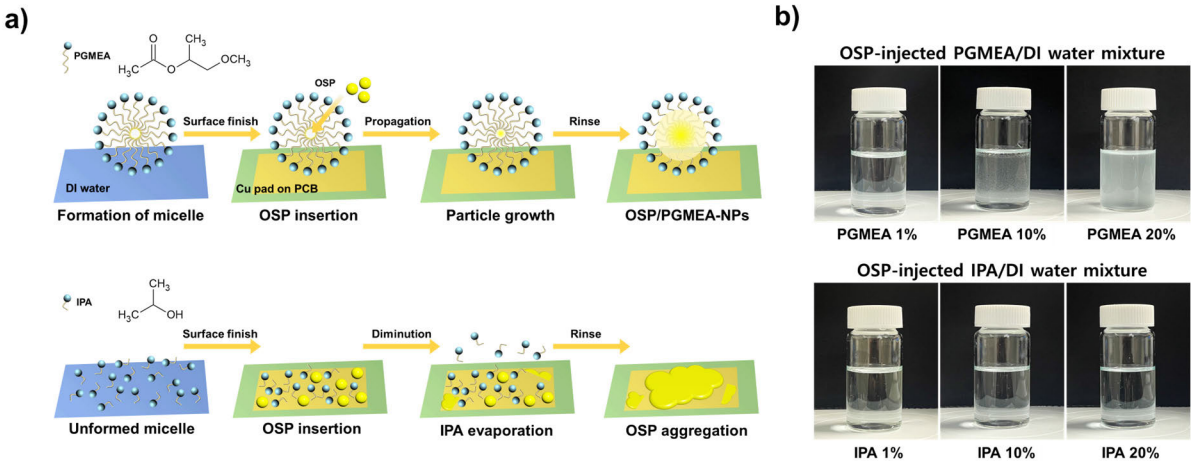

FIGURE 6. Schematic illustration for proposed mechanism of a) formation of unknown nanoparticles on the Cu pad using PGMEA and IPA solvents. b) Digital photographs of OSP-injected PGMEA and IPA mixtures.

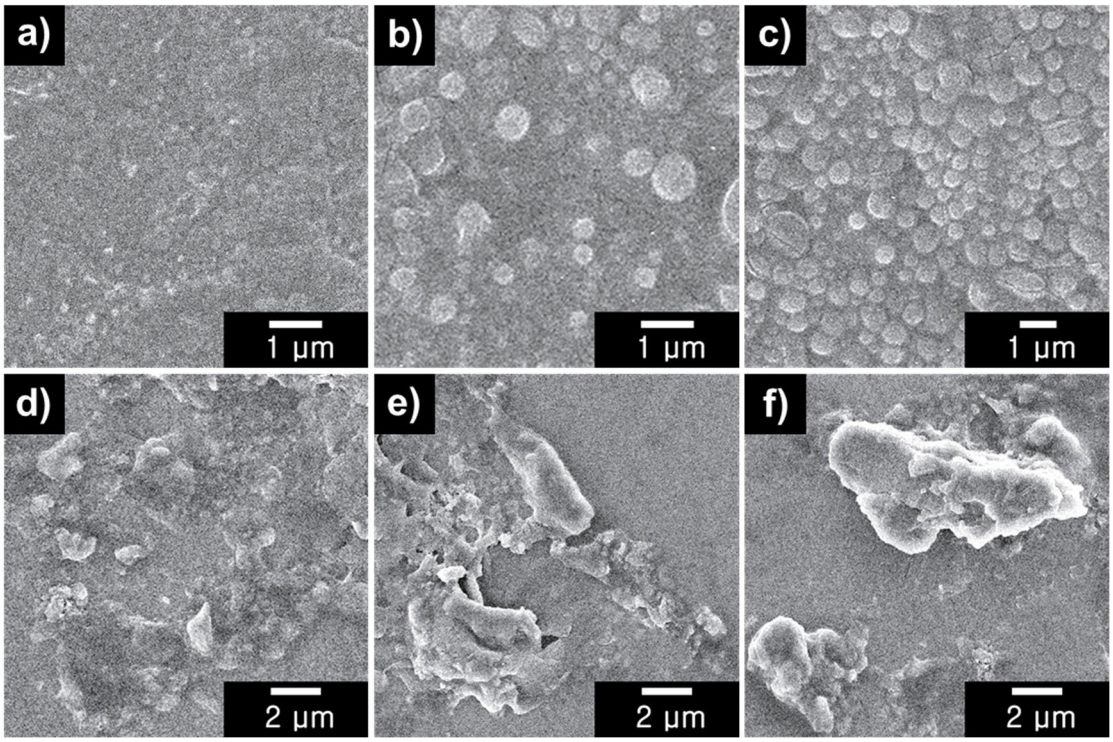

FIGURE 7. SEM micrographs of OSP-injected PGMEA mixtures of a) 1, b) 10, and c) 20 wt% concentrations, and OSP-injected IPA mixtures of d) 1, e) 10, and f) 20 wt% concentrations.

TABLE 1. Elemental composition of "OSP/PGMEA-NPs" and "OSP-finished Cu pad with unknown nanoparticles"[a].

Sample	Element (atomic %)			
	C	O	N	Cu
OSP/PGMEA-NPs	75.5	4.3	12.6	7.6
OSP-finished Cu pad with unknown nanoparticles	57.8	8.7	3.6	29.9

[a]Elemental compositions of samples was obtained using the EDS mode installed in the FE-SEM system (beam current: 10.0 μA, accelerating voltage: 20.0 kV).

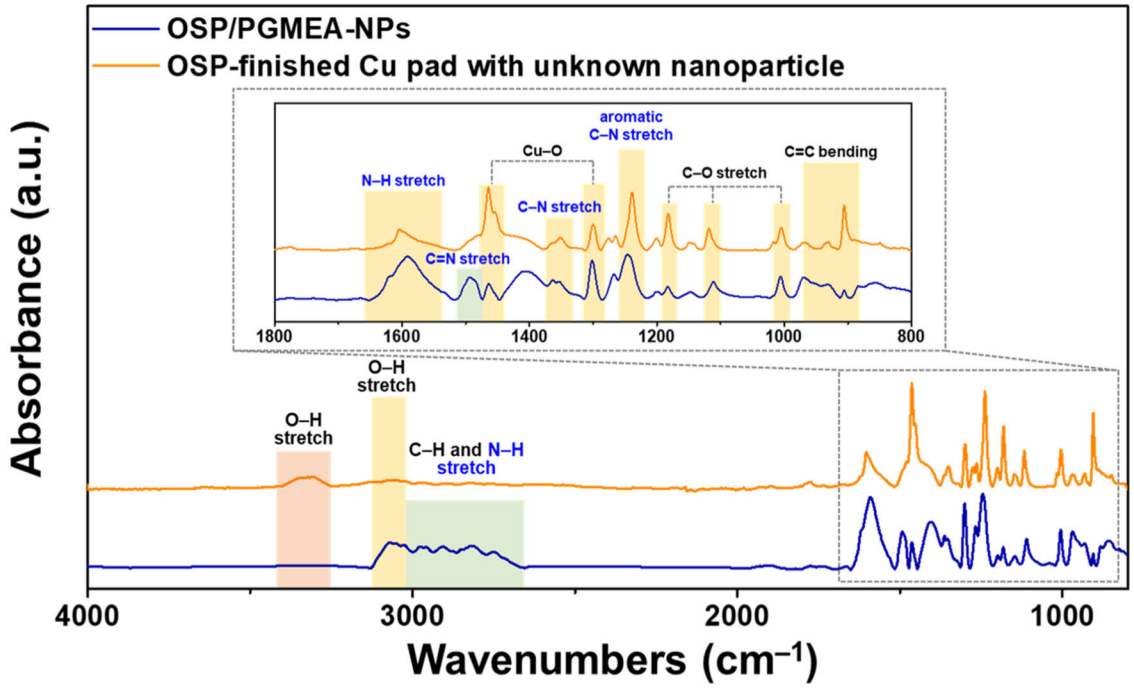

FIGURE 8. FT-IR spectra of OSP/PGMEA-NPs and OSP-finished Cu pad with unknown nanoparticles.

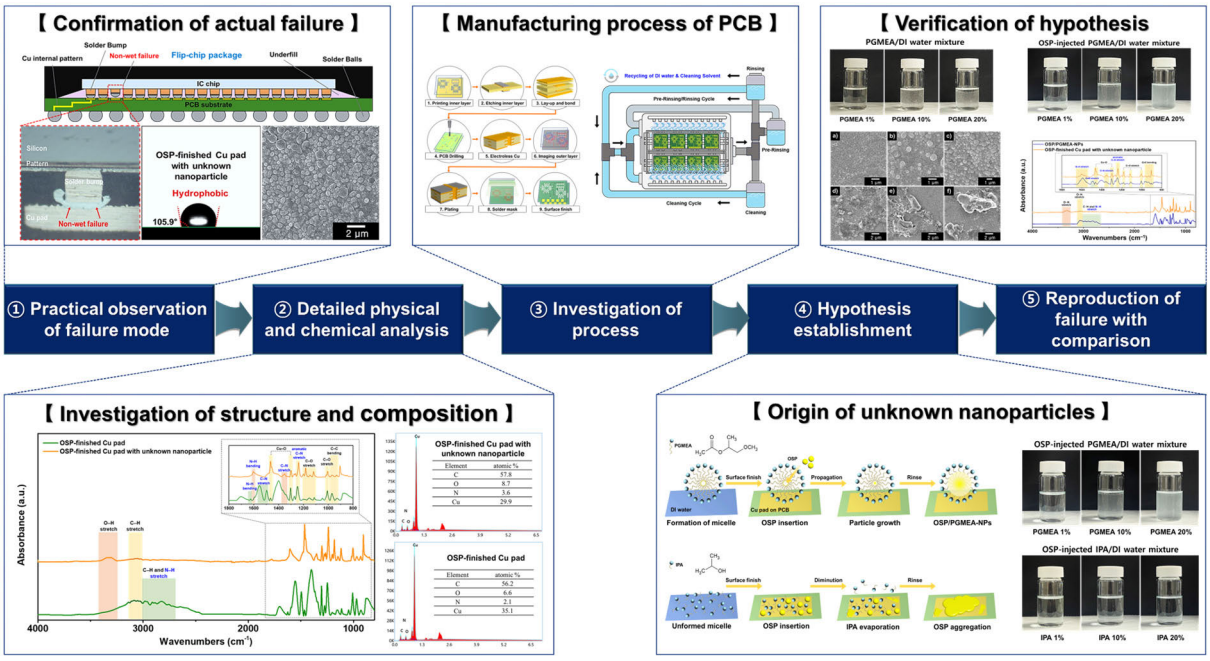

FIGURE 9. Overview of traceback analysis for failure identification in the semiconductor packaging process.

unknown nanoparticles originated from the PCB-cleaning process.

Thus, we concluded that the unknown nanoparticles were derived from the formation of emulsion and growth of OSP nanoparticles within the emulsion. The proposed mechanism for the formation of unknown nanoparticles in a practical PCB manufacturing process can be described as follows. First, the PCB was cleaned using PGMEA and DI water. During the cleaning process, recycled PGMEA and DI water were mixed in a cleaning bath or recycling pipe. Another option was that the remaining PGMEA or DI water could remain on the PCB and mix during the next cleaning process.

These mixed solvents could form emulsions because of their different polarities and remain on the PCB surface. Finally, the nanoparticles began to form in the emulsion on the Cu pad with the application of OSP for surface finishing. With hydrophobic nanoparticles, the Cu pad and solder bump could not form proper metal-to-metal bonds, resulting in the non-wet failure of the flip-chip package. Based on these results, we suggest that PCB manufacturers can prevent the formation of unknown nanoparticles by avoiding the mixing of solvents during the cleaning process or by applying plasma cleaning to remove the nanoparticles from the surface of the Cu pad. Accordingly, traceback analysis consisting of the five steps, *i.e.,* practical observation of failure mode; detailed physical and chemical analysis; investigation of process materials, and instrument; hypothesis establishment, and reproduction of failure with comparison successfully revealed the origin and mechanism of non-wet failure. The methodology and five steps of traceback analysis can be applied to identify another failure mode that occurs during the semiconductor manufacturing process. The methodology and summary of the traceback analysis are presented in Fig. 9.

IV. CONCLUSION

In this study, the origin of the unknown nanoparticles formed on the OSP-finished Cu pad of the PCB substrate, which facilitated the non-wet failure of the flip-chip package, was identified by applying traceback analysis. Traceback analysis was conducted in five steps: practical observation of the failure mode; detailed physical and chemical analysis; investigation of the process, materials, and instrument; hypothesis establishment; and reproduction of failure with comparison. In the reproduction of failure with the comparison step, PGMEA formed emulsions with DI water at concentrations of 10 and 20 wt%, as confirmed by visual or light scattering experiments. With OSP injection, OSP/PGMEA-NPs were reproduced in the emulsion, which had morphological and chemical characteristics similar to those of unknown nanoparticles. This result demonstrated that traceback analysis successfully determined the formation mechanism of unknown nanoparticles. To further develop and improve traceback analysis as a universal method, various failure cases from different companies must be studied. Despite this fact, most semiconductor-related manufacturing processes are non-disclosure; thus, this can be a limitation for current traceback analysis. However, we believe that the correct use and application of traceback analysis in industrial fields can effectively solve failures and identify their causes. Expanding this research to include other types of failures will provide a more comprehensive understanding of different mechanisms. Engaging with more industry partners will help gather diverse data and improve the robustness of this method.

ACKNOWLEDGMENT

(Ha-Yeong Kim and Jiwon Kim contributed equally to this work.)

REFERENCES

[1] N. B. Jaafar and C. S. Choong, "Establishment of highly dense wire bonding with insulated Au wire," in *Proc. IEEE 24th Electron. Packag. Technol. Conf. (EPTC)*, Dec. 2022, pp. 352–356.

[2] J. R. K. Marland, A. Tsiamis, D. Hoare, P. G. L. Lopez, S. L. Neale, J. R. Mercer, and S. Mitra, "Toward synthetic vascular graft monitoring using a flip-chip-on-flex impedance spectroscopy sensor," *IEEE Sensors J.*, vol. 23, no. 1, pp. 88–96, Jan. 2023.

[3] J. Lee, S. J. Kim, and B. Kim, "Development of a numerical simulation model for predicting the temperature of a flip-chip package during the laser-assisted bonding (LAB) process," in *Proc. 21st IEEE Intersociety Conf. Thermal Thermomechanical Phenomena Electron. Syst. (iTherm)*, May 2022, pp. 1–4.

[4] W. S. Tsai, C. Y. Huang, C. K. Chung, K. H. Yu, and C. F. Lin, "Generational changes of flip chip interconnection technology," in *Proc. 12th Int. Microsystems, Packag., Assem. Circuits Technol. Conf. (IMPACT)*, Oct. 2017, pp. 306–310.

[5] J. R. Lee, M. S. A. Aziz, M. H. H. Ishak, and C. Y. Khor, "A review on numerical approach of reflow soldering process for copper pillar technology," *Int. J. Adv. Manuf. Technol.*, vol. 121, nos. 7–8, pp. 4325–4353, Jul. 2022.

[6] K. Pun, M. N. Islam, and T. W. Ng, "ENEG and ENEPIG surface finish for long term solderability," in *Proc. 15th Int. Conf. Electron. Packag. Technol.*, Aug. 2014, pp. 1–5.

[7] L. Xu, S. Ling, Y. Lin, D. Li, S. Wu, and G. Zhai, "Fretting wear and reliability assessment of gold-plated electrical connectors," *Microelectron. Rel.*, vols. 100–101, Sep. 2019, Art. no. 113348.

[8] Z. Zhu, P. Ren, and H. Meng, "Electrodeposition of nanocrystalline au-cu alloy coatings with high hardness and corrosion resistance for electronic contact application," *Mater. Lett.*, vol. 330, Jan. 2023, Art. no. 133320.

[9] Y.-D. Jeon, Y.-B. Lee, and Y.-S. Choi, "Thin electroless Cu/OSP on electroless Ni as a novel surface finish for flip-chip solder joints," in *Proc. 56th Electron. Compon. Technol. Conf.*, pp. 119–124.

[10] J. Kim, S.-B. Jung, and J.-W. Yoon, "Effect of Ni(P) thickness in Au/Pd/Ni(P) surface finish on the electrical reliability of Sn–3.0Ag–0.5Cu solder joints during current-stressing," *J. Alloys Compounds*, vol. 850, Jan. 2021, Art. no. 156729.

[11] Y.-H. Wang, M. R. Howlader, K. Nishida, T. Kimura, and T. Suga, "Study on Sn–Ag oxidation and feasibility of room temperature bonding of Sn-Ag-Cu solder," *Mater. Trans.*, vol. 46, no. 11, pp. 2431–2436, Nov. 2005.

[12] S. N. Syed Nor, N. S. Rasanang, S. Karman, W. S. W. K. Zaman, S. W. Harun, and H. Arof, "A review: Surface plasmon resonance-based biosensor for early screening of SARS-CoV2 infection," *IEEE Access*, vol. 10, pp. 1228–1244, 2022.

[13] M. Riaz, U. Saeed, T. Mahmood, N. Abbas, and S. A. Abbasi, "An improved control chart for monitoring linear profiles and its application in thermal conductivity," *IEEE Access*, vol. 8, pp. 120679–120693, 2020.

[14] Y. Hou, L. Zhu, K. He, Z. Yang, S. Ma, and J. Lei, "Synthesis of three imidazole derivatives and corrosion inhibition performance for copper," *J. Mol. Liquids*, vol. 348, Feb. 2022, Art. no. 118432.

[15] J.-W. Peng, Y.-S. Chen, Y. Chen, J.-L. Liang, K.-L. Lin, and Y.-L. Lee, "Removed organic solderability preservative (OSPs) by Ar/O_2 microwave plasma to improve solder joint in thermal compression flip chip bonding," in *Proc. IEEE 64th Electron. Compon. Technol. Conf. (ECTC)*, May 2014, pp. 1584–1589.

[16] Z. P. Xiong, H. P. Sze, and K. H. Chua, "Bump non-wet issue in large-die flip chip package with eutectic Sn/Pb solder bump and SOP substrate pad," in *Proc. 6th Electron. Packag. Technol. Conf. (EPTC)*, Dec. 2004, pp. 438–443.

[17] P. Totsatitpaisan, K. Tashiro, and S. Chirachanchai, "Investigating the proton transferring route in a heteroaromatic compound Part I: A trial to develop Di- and trifunctional benzimidazole model compounds inducing the molecular packing structure with a hydrogen bond network," *J. Phys. Chem. A*, vol. 112, no. 41, pp. 10348–10358, Oct. 2008.

[18] M. A. Redayan, M. S. Hussein, and A. T. Lafta, "Synthesis, spectroscopic characterization, and antibacterial evaluation of new Schiff bases bearing benzimidazole moiety," *J. Phys., Conf. Ser.*, vol. 1003, May 2018, Art. no. 012018.

[19] C.-M. Yoon, Y. Jang, J. Noh, J. Kim, K. Lee, and J. Jang, "Enhanced electrorheological performance of mixed silica nanomaterial geometry," *ACS Appl. Mater. Interfaces*, vol. 9, no. 41, pp. 36358–36367, Oct. 2017.

[20] J. Kim, M. Kim, S. Cho, C. Yoon, C. Lee, J. Ryu, and J. Jang, "Multidimensional polyaniline/reduced graphene oxide/silica nanocomposite for efficient supercapacitor electrodes," *ChemNanoMat*, vol. 2, no. 3, pp. 236–241, Mar. 2016.
[21] C.-M. Yoon, G. Lee, J. Noh, C. Lee, O. J. Cheong, and J. Jang, "A comparative study of the electrorheological properties of various N-doped nanomaterials using ammonia plasma treatment," *Chem. Commun.*, vol. 52, no. 26, pp. 4808–4811, Mar. 2016.
[22] A. S. Kazachenko, E. Tanış, F. Akman, M. Medimagh, N. Issaoui, O. Al-Dossary, L. G. Bousiakou, A. S. Kazachenko, D. Zimonin, and A. M. Skripnikov, "A comprehensive study of N-Butyl-1H-Benzimidazole," *Molecules*, vol. 27, no. 22, p. 7864, Nov. 2022.
[23] M. R. Johan, M. S. M. Suan, N. L. Hawari, and H. A. Ching, "Annealing effects on the properties of copper oxide thin films prepared by chemical deposition," *Int. J. Electrochem. Sci.*, vol. 6, no. 12 pp. 6094–6104, Dec. 2011.
[24] M. Asandulesa, I. Topala, Y.-M. Legrand, S. Roualdes, V. Rouessac, and V. Harabagiu, "Chemical investigation on various aromatic compounds polymerization in low pressure helium plasma," *Plasma Chem. Plasma Process.*, vol. 34, no. 5, pp. 1219–1232, Sep. 2014.
[25] R. Sharma, M. A. Iqubal, S. Jheeta, and Kamaluddin, "Adsorption and oxidation of aromatic amines on metal(II) hexacyanocobaltate(III) complexes: Implication for oligomerization of exotic aromatic compounds," *Inorganics*, vol. 5, no. 2, p. 18, Mar. 2017.
[26] J. Kim, G. Lee, K. Lee, H. Yu, J. W. Lee, C.-M. Yoon, S. G. Kim, S. K. Kim, and J. Jang, "Fluorine plasma treatment on carbon-based perovskite solar cells for rapid moisture protection layer formation and performance enhancement," *Chem. Commun.*, vol. 56, no. 4, pp. 535–538, Jan. 2020.
[27] A. K. Alanazi, H. M. Abo-Dief, Z. A. Alothman, A. T. Mohamed, T. Pramanik, and A. M. Fallata, "Effect of rGO wt.% on the preparation of rGO/CuO nanocomposites at different test periods and temperatures," *Crystals*, vol. 12, no. 10, p. 1325, Sep. 2022.
[28] J. Liang, J. Jiang, M. Xu, X. Huo, D. Ye, S. Zhang, X. Wu, and W. Wu, "Improved lithium storage performance of urchin-like CuO microspheres by stereotaxically constructed graphene mediating synergistic effect," *J. Mater. Sci., Mater. Electron.*, vol. 32, no. 7, pp. 8557–8569, Mar. 2021.
[29] A. A. Anber, M. S. Essa, G. A. Kadhim, and S. S. Hashim, "Preparation of nanoparticles copper oxide using an atmospheric-pressure plasma jet," *J. Phys., Conf. Ser.*, vol. 1032, Jun. 2018, Art. no. 012009.
[30] K. Mallikarjuna, A. M. Al-Mohaimeed, D. A. Al-Farraj, L. V. Reddy, M. R. V. Reddy, and A. Mohammed, "Facile synthesis, characterization, anti-microbial and anti-oxidant properties of alkylamine functionalized dumb-bell shaped copper-silver nanostructures," *Crystals*, vol. 10, no. 11, p. 966, Oct. 2020.
[31] A. Ryan and H. Lewis, "Manufacturing an environmentally friendly PCB using existing industrial processes and equipment," *Robot. Comput.-Integr. Manuf.*, vol. 23, no. 6, pp. 720–726, Dec. 2007.
[32] C.-M. Yoon, Y. Jang, J. Noh, J. Kim, and J. Jang, "Smart fluid system dually responsive to light and electric fields: An electrophotorheological fluid," *ACS Nano*, vol. 11, no. 10, pp. 9789–9801, Oct. 2017.
[33] S. H. Yu, H. Jeon, H. Ko, J. H. Cha, S. Jeon, M. Jae, G.-H. Nam, K. Kim, Y. Gil, K. Lee, and D. S. Chung, "Polymer-based semiconductor wafer cleaning: The roles of organic acid, processing solvent, and polymer hydrophobicity," *Chem. Eng. J.*, vol. 470, Aug. 2023, Art. no. 144102.
[34] Y.-J. Park and G.-B. Lee, "Analysis of energy efficiency and productivity in dry process in PCB manufacturing," *Int. J. Precis. Eng. Manuf.*, vol. 14, no. 7, pp. 1213–1221, Jul. 2013.
[35] D. Liu, C. Li, X. Zhang, F. Yang, G. Sun, B. Yao, and H. Zhang, "Polarity effects of asphaltene subfractions on the stability and interfacial properties of water-in-model oil emulsions," *Fuel*, vol. 269, Jun. 2020, Art. no. 117450.
[36] D. Nagao, T. Ohta, H. Ishii, A. Imhof, and M. Konno, "Novel mini-reactor of silicone oil droplets for synthesis of morphology-controlled polymer particles," *Langmuir*, vol. 28, no. 51, pp. 17642–17646, Dec. 2012.
[37] D. K. Chelike and S. A. G. Thangavelu, "Biodegradable isocyanate-free polyurethane films via a noncatalytic route: Facile modified polycaprolactone triol and biobased diamine as precursors," *RSC Adv.*, vol. 13, no. 1, pp. 309–319, Dec. 2022.
[38] C.-M. Yoon, Y. Jang, S. Lee, and J. Jang, "Dual electric and magnetic responsivity of multilayered magnetite-embedded core/shell silica/titania nanoparticles with outermost silica shell," *J. Mater. Chem. C*, vol. 6, no. 38, pp. 10241–10249, Oct. 2018.
[39] U. Riaz, N. Nabi, F. R. Nwanze, and F. Yan, "Experimental and biophysical interaction studies of alanine modified polyaniline with bovine serum albumin and human serum albumin: Influence of alanine modification on the spectral, morphological and electronic properties," *Synth. Met.*, vol. 292, Jan. 2023, Art. no. 117248.
[40] J. Noh, S. Hong, C.-M. Yoon, S. Lee, and J. Jang, "Dual external field-responsive polyaniline-coated magnetite/silica nanoparticles for smart fluid applications," *Chem. Commun.*, vol. 53, no. 49, pp. 6645–6648, May 2017.
[41] D. Fan, W. Ma, L. Wang, J. Huang, J. Zhao, H. Zhang, and W. Chen, "Determination of structural changes in microwaved Rice starch using Fourier transform infrared and Raman spectroscopy," *Starch Stärke*, vol. 64, no. 8, pp. 598–606, May 2012.
[42] C.-M. Yoon, K. H. Cho, Y. Jang, J. Kim, K. Lee, H. Yu, S. Lee, and J. Jang, "Synthesis and electroresponse activity of porous polypyrrole/silica-titania core/shell nanoparticles," *Langmuir*, vol. 34, no. 51, pp. 15773–15782, Dec. 2018.
[43] S. Sudha, N. Sundaraganesan, M. Kurt, M. Cinar, and M. Karabacak, "FT-IR and FT-Raman spectra, vibrational assignments, NBO analysis and DFT calculations of 2-amino-4-chlorobenzonitrile," *J. Mol. Struct.*, vol. 985, nos. 2–3, pp. 148–156, Jan. 2011.

HA-YEONG KIM received the B.S. degree in chemical and biological engineering from Hanbat National University, Daejeon, South Korea, in 2023. Her research interest includes semiconductor packaging materials.

JIWON KIM received the B.S. degree in chemical and biological engineering from Hanbat National University, Daejeon, South Korea, in 2023. Her research interest includes the designing and fabrication of smart materials for various applications.

YEON-RYONG CHU received the B.S. degree in chemical and biological engineering from Hanbat National University, Daejeon, South Korea, in 2023. His research interest includes semiconductor packaging materials.

SUK JEKAL received the M.S. degree in chemical and biological engineering from Hanbat National University, Daejeon, South Korea, in 2024. His research interests include electrochemistry and semiconductor packaging.

MINKI SA received the B.S. degree in chemical and biological engineering from Hanbat National University, Daejeon, South Korea, in 2024. His research interest includes synthesis of various nanomaterials.

CHAN-GYO KIM received the B.S. degree in chemical and biological engineering from Hanbat National University, Daejeon, South Korea, in 2023. His research interests include semiconductor devices, lithium-ion battery, supercapacitor, and reliability testing.

GYU-SIK PARK received the B.S. degree in chemical and biological engineering from Hanbat National University, Daejeon, South Korea, in 2024. His research interest includes semiconductor packaging materials.

JISU LIM received the B.S. degree in chemical and biological engineering from Hanbat National University, Daejeon, South Korea, in 2024. Her research interest includes semiconductor packaging materials.

ZAMBAGA OTGONBAYAR received the Ph.D. degree in engineering from Hanseo University, South Korea, in 2023. Her main research interest includes CO_2 reduction through photoelectrochemical method. Her current research interests include LiDAR-reflective material, nanoadditive, and energetic materials.

CHANG-MIN YOON received the B.S. degree from Pennsylvania State University, University Park, USA, in 2013, and the Ph.D. degree from Seoul National University, Seoul, South Korea, in 2018. He joined Samsung Electronics, in 2018. He was a Staff Engineer with the DS Division for three years. In 2021, he became a Professor with the Department of Chemical and Biological Engineering, Hanbat National University. His current research interests include smart fluids, electrochemistry, and semiconductor packaging materials.